

# Geophysical Research Letters®

## RESEARCH LETTER

10.1029/2025GL114934

### Key Points:

- The 2019 and 2022 droughts caused marked reductions in photosynthetic activity and ozone uptake by vegetation in China
- This worsened air pollution extremes, leading to a threefold increase in high-ozone events above 100 ppbv
- The linkage between soil moisture droughts and ozone extremes can be exploited to improve ozone forecasts for public health warnings

### Supporting Information:

Supporting Information may be found in the online version of this article.

### Correspondence to:

M. Lin,  
Meiyun.Lin@noaa.gov

### Citation:

Lin, M., Xie, Y., De Smedt, I., & Horowitz, L. W. (2025). Ozone pollution extremes in Southeast China exacerbated by reduced uptake by vegetation during hot droughts. *Geophysical Research Letters*, 52, e2025GL114934. <https://doi.org/10.1029/2025GL114934>

Received 16 JAN 2025

Accepted 4 APR 2025

### Author Contributions:

**Conceptualization:** Meiyun Lin

**Data curation:** Meiyun Lin, Yuanyu Xie, Isabelle De Smedt

**Formal analysis:** Meiyun Lin

**Investigation:** Meiyun Lin

**Methodology:** Meiyun Lin

**Validation:** Meiyun Lin

**Writing – original draft:** Meiyun Lin

**Writing – review & editing:** Meiyun Lin, Larry W. Horowitz

© 2025. The Author(s).

This is an open access article under the terms of the [Creative Commons Attribution-NonCommercial-NoDerivs License](#), which permits use and distribution in any medium, provided the original work is properly cited, the use is non-commercial and no modifications or adaptations are made.

## Ozone Pollution Extremes in Southeast China Exacerbated by Reduced Uptake by Vegetation During Hot Droughts

Meiyun Lin<sup>1</sup> , Yuanyu Xie<sup>2</sup> , Isabelle De Smedt<sup>3</sup> , and Larry W. Horowitz<sup>1</sup> 

<sup>1</sup>NOAA Geophysical Fluid Dynamics Laboratory, Princeton, NJ, USA, <sup>2</sup>Princeton School of Public Policy and International Affairs, Princeton University, Princeton, NJ, USA, <sup>3</sup>Royal Belgian Institute for Space Aeronomy (BIRA-IASB), Brussels, Belgium

**Abstract** Using a decade of observations and chemistry-climate model simulations (2014–2023), we highlight the key role of biosphere-atmosphere interactions in driving late summer–autumn ozone pollution extremes over Southeast China during hot droughts. In the 2019 and 2022 droughts, stomatal closure in the Yangtze River Basin, caused by soil moisture deficits, led to ~60% reductions in ozone deposition rates to vegetation, aligning with reduced photosynthesis inferred from satellite remote sensing of solar induced fluorescence. Ozone production increased due to higher isoprene emissions from heat stress, NO<sub>x</sub>-rich airflow from North China, and enhanced solar radiation. Soil drought intensified temperatures and increased isoprene emissions by 27%, but these only had marginal impact on ozone (<5 ppbv) in South China, where ozone formation is NO<sub>x</sub>-limited. Reduced ozone uptake by drought-stressed vegetation played a dominant role, driving 10–20 ppbv increases in daily maximum 8-hr average ozone concentrations and a threefold rise in events exceeding 100 ppbv.

**Plain Language Summary** Ozone pollution is a major problem in China, affecting both health and the environment. This study shows that the worst ozone pollution in Southeast China is linked to droughts and heatwaves in late summer and autumn. When plants experience soil moisture drought, they close small pores in their leaves to save water, which reduces their ability to absorb ozone, causing higher ozone levels in the air. During the record-setting droughts of 2019 and 2022, the lack of ozone uptake by stressed plants led to a threefold rise in high-ozone events over 100 ppbv, which is well above China's air quality limit of 80 ppbv. This significant impact of drought on ozone air quality was unknown in the region before and is important to understand as droughts and heatwaves may become more common in a warming climate. Recognizing the link to soil moisture drought can improve ozone forecasts and help with public health warnings.

## 1. Introduction

High concentrations of ozone in surface air are hazardous to human lungs and have been blamed for tens of billions of dollars in annual agricultural loss in China (e.g., Feng et al., 2022; Mao et al., 2024). Transport of Asian ozone pollution contributed to increases in western US background ozone during the 1980s–2000s (e.g., Jaffe et al., 2018; Lin et al., 2012, 2015, 2017). Over the past decade, substantial effort has been invested in controlling emissions of SO<sub>2</sub>, NO<sub>x</sub>, and carbonaceous aerosols with the aim of reducing PM<sub>2.5</sub> levels in China (Q. Zhang et al., 2019). The nationwide monitoring network reveals marked improvements in PM<sub>2.5</sub> air quality since 2014, however, severe ozone pollution persists in China despite NO<sub>x</sub> emission controls (Lu et al., 2018; T. Wang et al., 2017). A number of studies have examined the influence of heterogeneous chemistry, ozone production regimes, heatwaves, and the temperature-driven biogenic emissions (e.g., Li et al., 2019, 2020; Z. Liu et al., 2021; Ma et al., 2019; N. Wang et al., 2022; P. Wang et al., 2022). Little is known about the role of compound drought and heat events (also termed hot droughts), which may become more prevalent in the context of global warming (e.g., Trenberth et al., 2014).

When plants are under drought stress, leaf stomata close to prevent water loss, inhibiting photosynthesis and limiting the uptake of ozone by vegetation (an important component of dry deposition) (Clifton et al., 2020; Lin et al., 2019). The impact of drought-induced reductions in ozone removal is less studied compared to isoprene-induced ozone production, partly because the commonly used Wesely (1989) dry deposition scheme does not account for stomatal closure caused by soil drying (see Lin et al. (2019) for a review). Reductions in ozone removal by vegetation, caused by more frequent hot droughts, have been identified as a major climate penalty feedback that

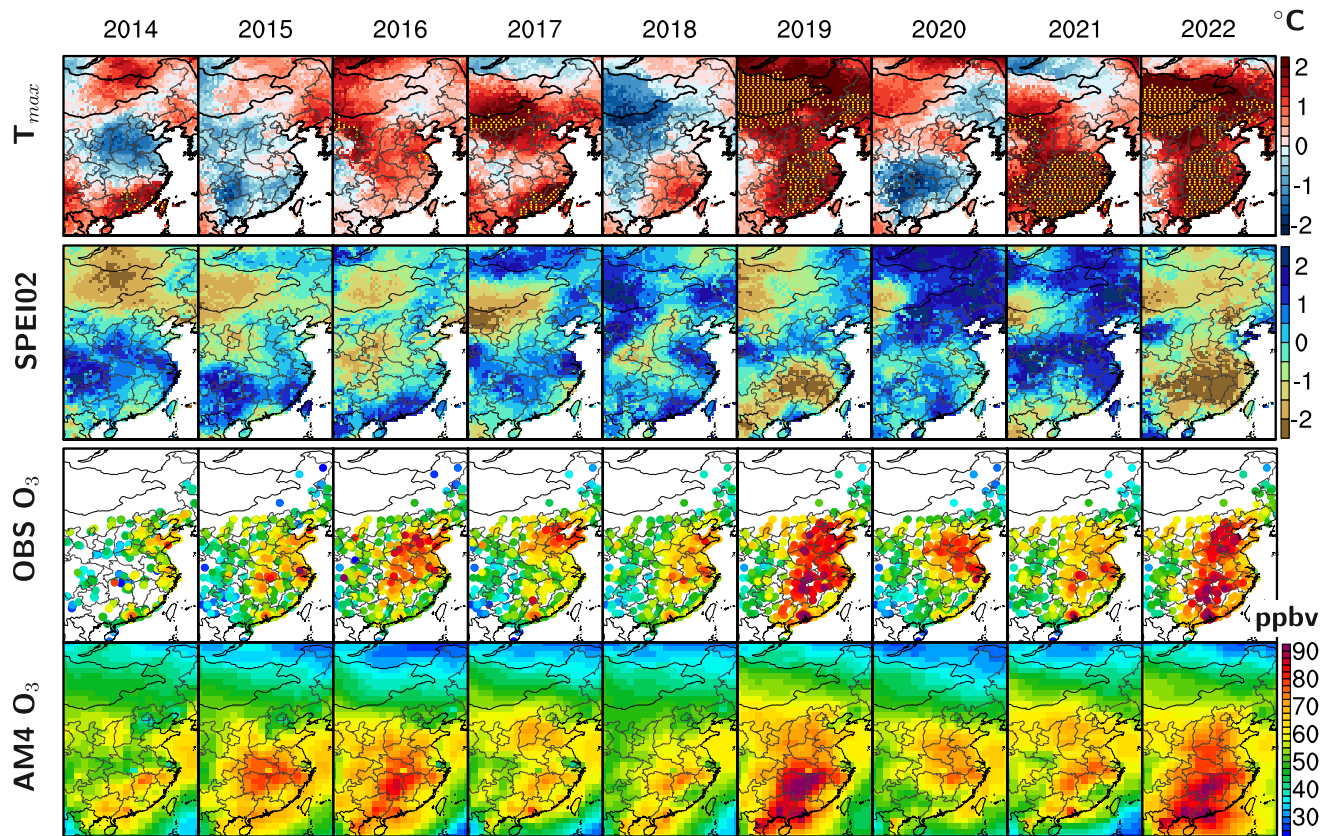


**Figure 1.** Maps of observed anomalies in September mean daily maximum temperature ( $T_{\max}$ , with stippling indicating two standard deviations warmer than the 1981–2010 average), Standardized Precipitation Evapotranspiration Index integrated over August–September (SPEI02), and September mean surface MDA8  $O_3$  concentrations from observations and model simulations (AM4\_drySoil) from 2014 to 2022.

contributes to the persistence of surface ozone pollution over Europe in recent decades, according to new observations and models (Lin et al., 2020). Limitation in ozone uptake by vegetation has also been reported for severe droughts in the US (e.g., Huang et al., 2016; Lin et al., 2017, 2019). The Yangtze River Basin (YRB), home to over 400 million people in China, experienced a number of droughts in recent years, including the record-setting hot droughts of 2019 and 2022 (L. Chen et al., 2023; Z. Liu & Zhou, 2021; Y. Liu et al., 2023; Ma et al., 2022). Severe ozone pollution, above one standard deviation in the 10-year observational record, was measured across eastern China during late summer–fall of 2019 and 2022 (Figure 1 and Figure S1 in Supporting Information S1).

Here we probe the underlying mechanisms driving the observed ozone extremes during hot droughts in China. In contrast to the North China Plain where surface ozone peaks seasonally in late spring–early summer (June), ozone pollution in the Yangtze Plain and the Pearl River Basin over Southeast China peaks in late summer–fall (September) (Figure S1 in Supporting Information S1). During June–August, Southeast China experiences lower ozone as a consequence of increased cloudiness from the East Asian Summer Monsoon and the monsoonal intrusion of low-ozone air from the tropical Pacific (Lin et al., 2009; H. Y. Liu et al., 2002; Y. Wang et al., 2008; W. Wang et al., 2022). Southeast China also features a wide coverage of forest ecosystems, providing favorable conditions for biosphere–atmosphere interactions. Using a suite of observations and chemistry–climate model simulations, we assess the contributions from land–atmosphere coupling, changes in ozone removal by vegetation, biogenic isoprene emissions and their interactions with anthropogenic  $NO_x$  for ozone production.

## 2. Methods: Observations and Model Simulations

We calculate maximum daily 8-hr average ozone (MDA8  $O_3$ ) concentrations using hourly measurements during 2014–2023 from China's national air quality monitoring network (Text S1 in Supporting Information S1). To investigate correlations between ozone and hot drought, we use version 4.08 of the Climate Research Unit

monthly  $0.5^\circ \times 0.5^\circ$  gridded daily maximum 2 m temperature ( $T_{\max}$ ) (Harris et al., 2020) and version 2.10 of the Standardized Precipitation Evapotranspiration Index (SPEI) database (Begueria et al., 2014). SPEI is a multi-scalar drought index considering the combined effects of precipitation and temperature; in this study we use SPEI02 that integrates water status over the preceding two months. We also analyze 500 hPa geopotential heights, 850 hPa winds, and surface downward shortwave radiation from the ERA-5 monthly mean reanalysis.

To investigate changes in vegetation after exposure to drought, we analyze satellite remote sensing of Solar Induced Fluorescence (SIF), a measurement of the small amounts of radiation emitted by chlorophyll in plants during photosynthesis (X. Chen et al., 2022; Guanter et al., 2021; Helm et al., 2020). To examine anomalies in isoprene emissions from vegetation, we analyze tropospheric column densities of formaldehyde ( $\Omega_{\text{HCHO}}$ ), a high-yield isoprene oxidation product (Millet et al., 2008; Palmer et al., 2003; Zheng et al., 2017). Both  $\Omega_{\text{HCHO}}$  and SIF have been retrieved from the TROPOspheric Monitoring Instrument (TROPOMI) on board the Copernicus Sentinel-5P satellite since 2018 (De Smedt et al., 2021; Guanter et al., 2021). We also use the weekly Vegetation Health Index (VHI) products from the Visible Infrared Imaging Radiometer Suite (VIIRS) onboard the Suomi-NPP (2013–2020) and NOAA-20 (2021–2023) satellites (National Environmental Satellite, Data, and Information Service, 2024).

We conduct a set of 16-year hindcast simulations (2008–2023) with GFDL's Atmospheric and Land Model AM4/LM4 at  $\sim 100 \times 100 \text{ km}^2$  horizontal resolution (Horowitz et al., 2020), with updates to interannually varying anthropogenic and biomass burning emissions, atmospheric chemistry, and dry deposition schemes following Lin, Horowitz, Zhao, et al. (2024) and Lin, Horowitz, Hu, and Permar (2024). One novel feature of AM4/LM4 used here is a mechanistic simulation of ozone deposition velocities ( $V_{\text{d},\text{O}_3}$ ) to vegetation depending on photosynthesis, soil water stress, and atmospheric  $\text{CO}_2$  concentration (Lin et al., 2019, 2020). The limitation imposed by soil water stress is determined by the ratio of water supply from soil-root interface to the transpiration demand at non-water-limited stomatal conductance, as simulated in our dynamic vegetation land model. Two model configurations are analyzed in this study: one with soil types and parameters taken from LM3.0 (Milly et al., 2014; Paulot et al., 2018) and the other with soil types and parameters taken from LM4.0 (Held et al., 2019; Zhao et al., 2018, Text S2 in Supporting Information S1). Through nudging to horizontal winds from the NOAA Global Forecast System, the two experiments share large-scale atmospheric circulation while simulating soil moisture, temperature, and precipitation interactively. Both experiments capture low rainfall in September 2019 and 2022 over Southeast China but they exhibit different soil water holding capacity (Figure S2 in Supporting Information S1). The LM4.0 soil configuration (hereafter **AM4\_wetSoil**) simulates  $\sim 27\%$  higher soil moisture levels than the LM3.0 soil configuration (hereafter **AM4\_drySoil**) over Southeast China (Figure S3 in Supporting Information S1). When soil moisture levels decrease below a critical threshold, as occurred during the 2019 and 2022 droughts in AM4\_drySoil, significant stomatal closure is triggered to conserve water, limiting the intake of  $\text{CO}_2$  for photosynthesis and the stomatal uptake of ozone by vegetation. Ozone flux measurements worldwide confirm that our dry deposition scheme captures key  $V_{\text{d},\text{O}_3}$  features, including spatial, seasonal, and interannual variability due to soil water stress (Lin et al., 2019).

In all simulations, biogenic isoprene emissions increase at higher solar radiation and temperature, following the Model of Emissions of Gases and Aerosols from Nature (MEGAN) (Guenther et al., 2012), with updates to land cover and emission potentials as in Lin, Horowitz, Zhao, et al. (2024). The implementation of MEGAN in AM4 does not include a direct dependency on soil moisture. As we will discuss later, soil dryness affects surface air temperature and therefore the temperature-driven isoprene emissions. To isolate the effects of changes in ozone removal efficiency during drought, we conduct a third simulation using the same soil configuration as **AM4\_drySoil** but with dry deposition velocities ( $V_{\text{d}}$ ) of ozone and other reactive gases held constant at 2018 monthly values (hereafter **FIXDEPV**).

### 3. Observed Correlations Between Hot Drought and Ozone Pollution

Using observations, we first demonstrate correlations between surface air temperature, drought, and ozone pollution in eastern China during late summer–fall (Figure 1). The observed year-to-year variability and spatial pattern of late summer ozone pollution over Southeast China show strong correlations with drought conditions, and to a lesser extent with surface air temperature. Lower ozone levels were observed during cooler and wetter conditions in September 2014, 2015, 2017, and 2018. The highest ozone concentrations were observed in the Yangtze Plain and the Pearl River Basin during the compound heatwave and drought events of September 2019

and 2022. The magnitude and spatiotemporal persistence of late summer high-ozone pollution during these two years is unprecedented over the 10-year observational record. The percentage of site-days with MDA8 O<sub>3</sub> exceeding 80 ppbv (approximately 160 µg/m<sup>3</sup>—the Chinese National Ozone Air Quality Standard) is 29% in 2019 and 2022, compared to 10% on average for the other years.

While many recent studies have discussed ozone pollution in China being exacerbated by high temperatures (e.g., Li et al., 2020; N. Wang et al., 2024; P. Wang et al., 2022; Xia et al., 2022), we distinguish the effects of humid versus dry heat extremes. September 2021 is an example of a humid heatwave associated with a westward extension of the Western Pacific Subtropical High (Ding et al., 2022; D.-Q. Wang & Sun, 2022), which brought rain-bearing, low-O<sub>3</sub> air from the tropical Pacific to South China (Figure S5 in Supporting Information S1). Despite that surface air temperature in South China in September 2021 was two standard deviations warmer than the 1981–2010 average, ozone was not significantly enhanced. Abundant water vapor enhanced ozone chemical loss, while persistent rainfall maintained soil moisture, supporting vegetation that removed ozone efficiently via stomatal uptake. In contrast, late summer–autumn 2019 saw an extreme drought in eastern China, marked by prolonged dryness and record intensity. This event was driven by the meridionally elongated cyclonic circulation anomalies over the western North Pacific and the enhanced northerly wind anomalies over eastern China (L. Chen et al., 2023; Z. Liu & Zhou, 2021, Figure S5 in Supporting Information S1). The drought began in the Yangtze Plain in August–September and extended into South China through November. Deterioration of ozone air quality in the Pearl River Delta (PRD) manifested as an expansion of the ozone season in 2019, with monthly mean MDA8 O<sub>3</sub> consistently above 70 ppbv and above one standard deviation from September to November (Figure S1 in Supporting Information S1). The 2022 drought was more severe than the 2019 drought (Figure 1), and was characterized by rapid intensification (Y. Liu et al., 2023; Ma et al., 2022; L. Zhang et al., 2023). As drought intensified, ozone pollution increased rapidly in the Yangtze Plain during September 2022 and in the PRD during September–October 2022 (Figure S1 in Supporting Information S1).

#### 4. Reduced Ozone Removal by Drought-Stressed Vegetation

Using satellite observations and model simulations, we show soil water stress reduced vegetation health, photosynthesis, and ozone uptake by vegetation (Figure 2). During 23–30 September 2019, the VIIRS VHI was well below 36 in the Yangtze Plain (Hubei and Henan), indicating levels of vegetation stress, losses of crop, and pasture production (Figure 2a). In contrast, the indices were well above 60 during 23–30 September 2017 under wetter conditions (Figure 1), indicating favorable conditions for plentiful growth. Figure 2b compares TROPOMI SIF, a key indicator of a plant's photosynthetic activity, under normal conditions (average of 2018, 2020, 2021, and 2023) versus under drought stress in 2019 and 2022. SIF exhibits pronounced reductions (exceeding one standard deviation) in the Middle Reaches of the Yangtze Plain during September 2019, consistent with deterioration of vegetation health. During September 2022, the SIF reduction expanded to a larger land area, including Sichuan-Chongqing, Guizhou, Hubei, and Hunan in the Upper-Middle Yangtze Plain, consistent with drought stress in these areas.

Figures 2c and 2d shows daytime (9 a.m.–3 p.m. local time) ozone deposition rates averaged over all vegetation types for 20–30 September 2019 and 2022 versus 2017 from two AM4 simulations with different soil water availability. In AM4\_drySoil, daytime  $V_{d,O_3}$  over the Yangtze plain decreased to 0.2–0.4 cm s<sup>−1</sup> in 2019 and 2022, representing a 60% reduction from 0.5 to 0.7 cm s<sup>−1</sup> under wet conditions in 2017, primarily due to the limitation of stomatal conductance under soil water stress (Figure S3 in Supporting Information S1). With higher soil moisture in AM4\_wetSoil, stomatal closure was not triggered and simulated  $V_{d,O_3}$  did not show significant changes in 2019/2022 compared to 2017. The very low  $V_{d,O_3}$  values (0.2–0.4 cm s<sup>−1</sup>) simulated in AM4\_drySoil for Southeast China in 2022 agrees with those derived from ozone flux measurements at forest sites during the European mega-drought of 2003 and the North American mega-drought of 2012 (Lin et al., 2019, 2020). Further supporting our model results, AM4\_drySoil simulated areas with the most pronounced  $V_{d,O_3}$  decreases are consistent with satellite observations of the vegetated areas with reductions in photosynthesis.

#### 5. Increased Isoprene Emissions and Ozone Production

TROPOMI observed a 30% increase of  $\Omega_{HCHO}$  in forested regions over Southeast China during September 2019 (Figure 3a) and 2022 (Figures S6 and S7 in Supporting Information S1). Increases in biogenic isoprene emissions and  $\Omega_{HCHO}$  are seen over Southeast China in AM4\_drySoil simulations with MEGAN (Figures 3b and 3c).



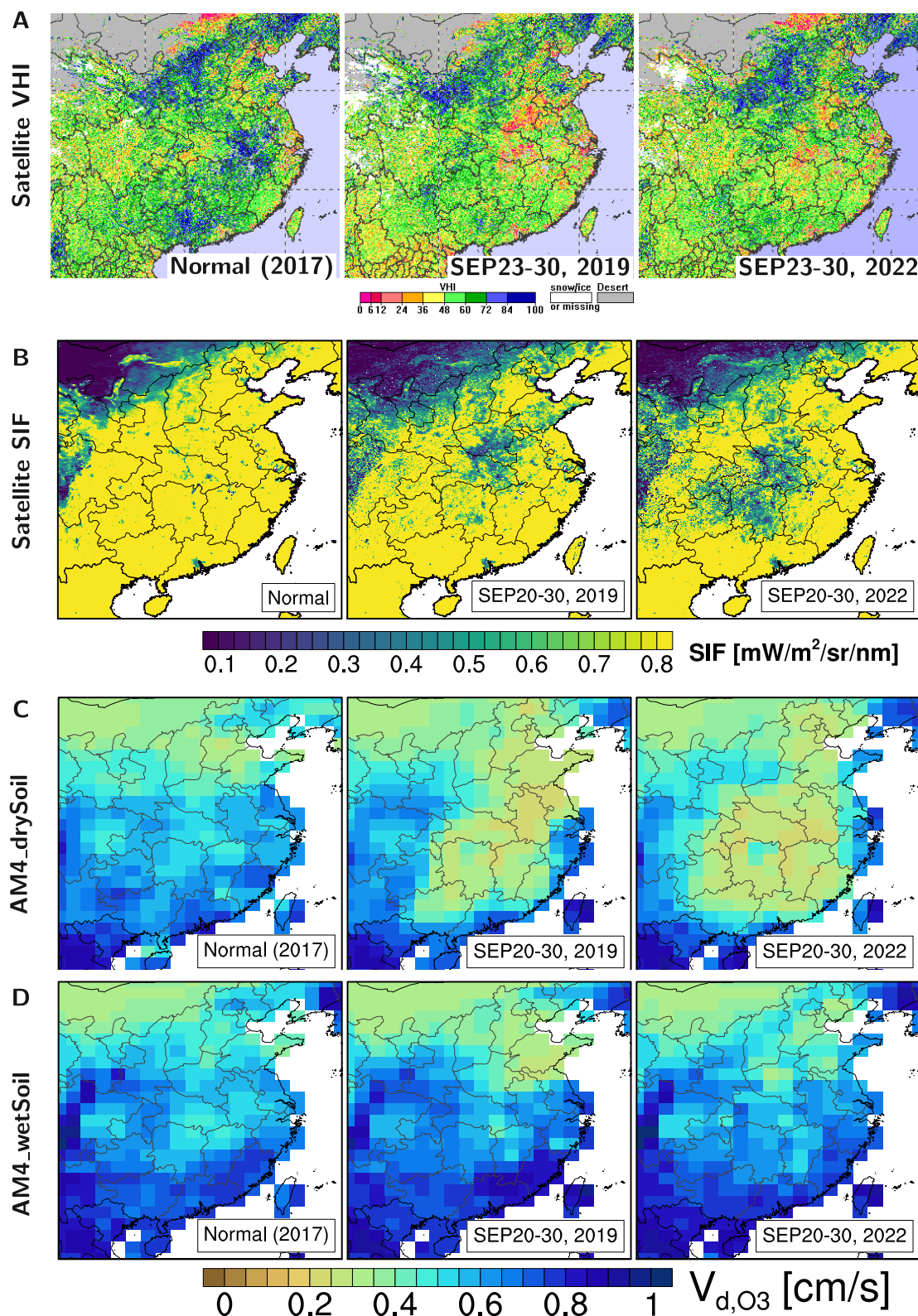


**Figure 2.** Comparison of data from normal conditions (2017) and drought conditions (2019 and 2022) in September for: (a) Visible Infrared Imaging Radiometer Suite Vegetation Health Index, (b) TROPOspheric Monitoring Instrument (TROPOMI) Solar Induced Fluorescence, and (c, d) Simulated daytime ozone dry deposition velocities ( $V_{d,O3}$ ) from the AM4\_drySoil and AM4\_wetSoil experiments. Note that TROPOMI data for 2017 is unavailable, so the average of data from 2018, 2020, 2021, and 2023 is used to represent normal conditions.

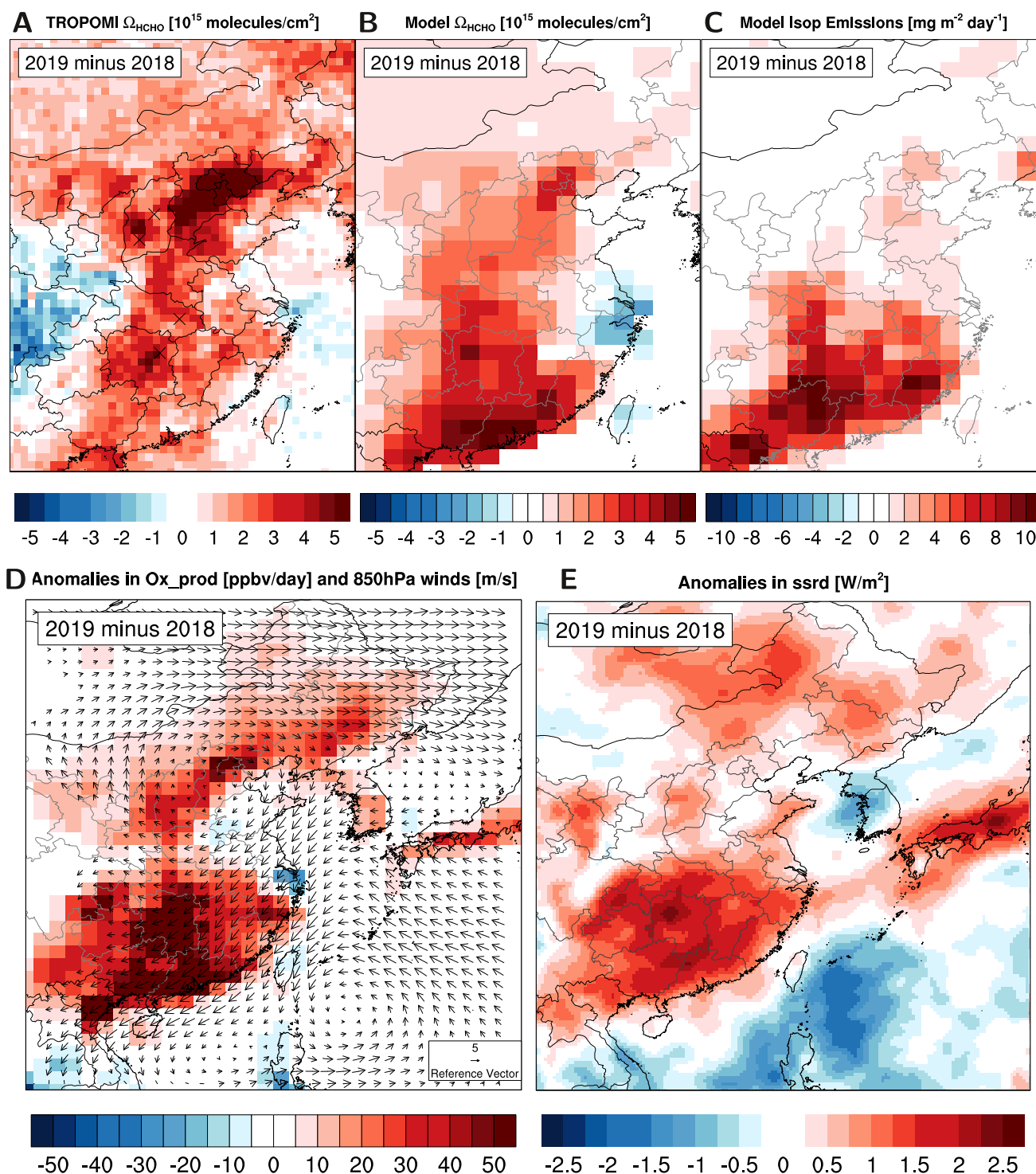


**Figure 3.** Anomalies in September 2019 relative to 2018 for: (a, b) Satellite-retrieved and AM4\_drySoil simulated tropospheric column densities of formaldehyde ( $\Omega_{\text{HCHO}}$ ), (c) Simulated biogenic isoprene emissions, (d) Simulated ozone (odd oxygen) production rates overlaid with 850 hPa winds, and (e) ERA5-observed surface downward shortwave radiation.

Simulated  $\Omega_{\text{HCHO}}$  has a large bias against TROPOMI over North China, which may reflect uncertainties in anthropogenic VOC emissions or in the land cover data set used by MEGAN (e.g., Ma et al., 2019; Pu et al., 2022). A few studies reported sustained drought stress leading to decreased isoprene emissions based on flux measurements at a temperate forest during the 2012 U.S. drought (Opacka et al., 2022; Seco et al., 2015;

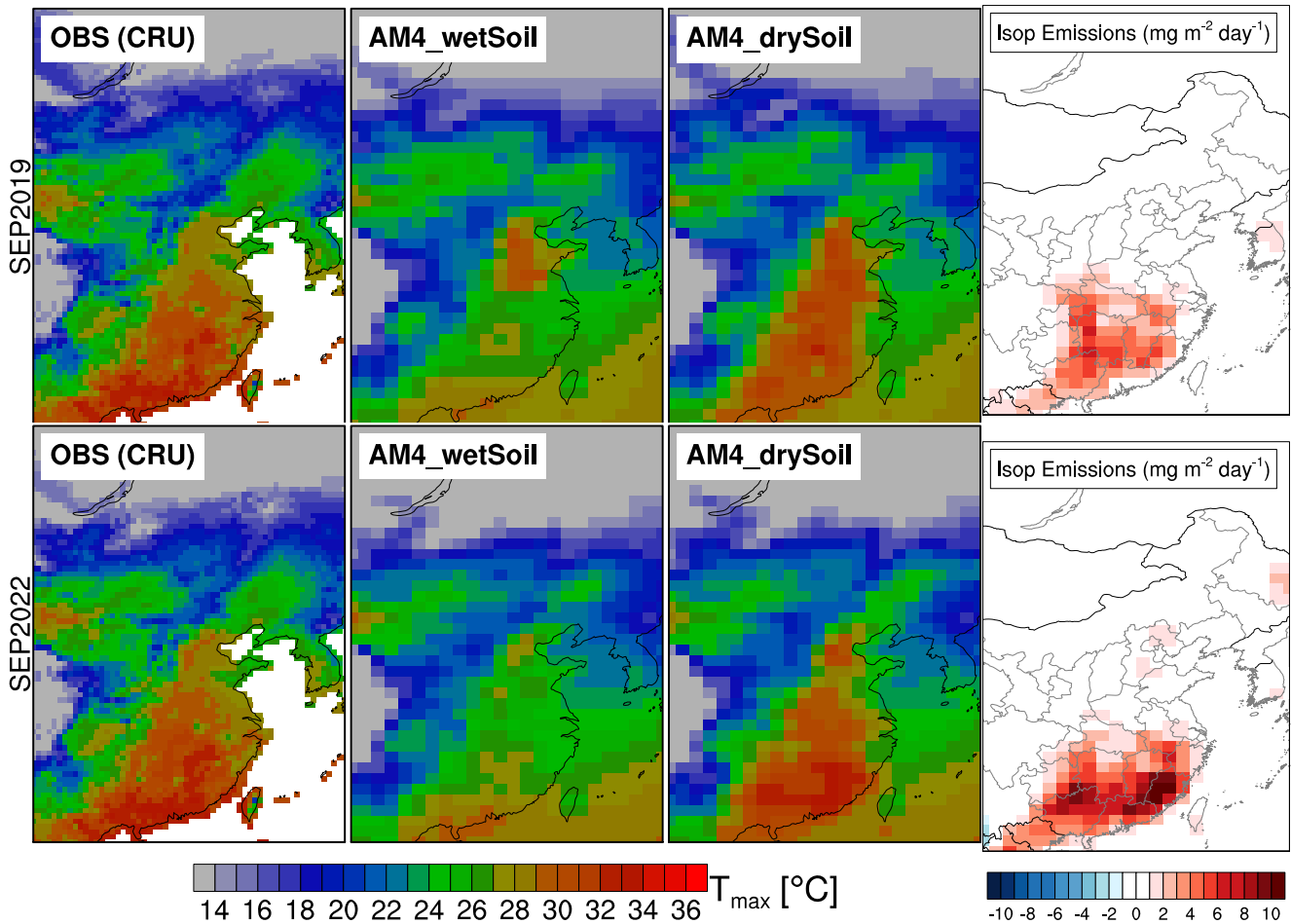


**Figure 4.** Monthly mean  $T_{\max}$  for September 2019 and 2022 from observations and model simulations with different soil moisture levels, along with the impact (drySoil minus wetSoil) on biogenic isoprene emissions.

Shutter et al., 2024; Zheng et al., 2017). For Southeast China, however, TROPOMI  $\Omega_{\text{HCHO}}$  reveals little evidence of a drought suppression effect. For both September 2019 and 2022, the areas with the largest  $\Omega_{\text{HCHO}}$  increases over Southeast China correspond to the areas with positive anomalies in  $T_{\max}$ , indicating that the response of isoprene emissions to heat stress is the main driver for these  $\Omega_{\text{HCHO}}$  increases detected from space. Positive  $\Omega_{\text{HCHO}}$  anomalies were also observed during the 2005 Amazon drought and the 2010 Russian heatwave and drought (Marengo et al., 2008; Morfopoulos et al., 2022). Isoprene emissions can continue at a high rate even when carbon assimilation is reduced due to stomatal closure (Sharkey & Monson, 2014).

Land-atmosphere interactions have been recognized as a key reason for the amplification and persistence of heatwaves (e.g., Teuling, 2018). Sensitivity simulations with AM4 show that dry soils warm the atmosphere and thereby amplify the temperature-driven increase in isoprene emissions over South China during September 2019 and 2022 (Figure 4). Monthly mean  $T_{\max}$  increases by 2°C–3°C from AM4\_wetSoil to AM4\_drySoil, leading to better agreements with observations. Isoprene emissions in AM4\_drySoil increase by 27% (2–6 mg m<sup>-2</sup> day<sup>-1</sup>) on average over Southeast China.

Figures 3d and 3e displays anomalies in  $\text{O}_x$  (odd oxygen) production rates in AM4\_drySoil, 850 hPa wind vectors, and surface downward shortwave radiation for September 2019. In contrast to 2017 and 2021 when southerly winds bring rain-bearing, low- $\text{NO}_x$  air from the tropical Pacific to most of south China, the overwhelming northerly winds during September 2019 and 2022 bring dry and  $\text{NO}_x$ -rich air from the highly industrialized North China Plain to south China. Transported anthropogenic  $\text{NO}_x$  likely interacted with increased isoprene emissions from vegetation to accelerate in situ ozone production in the presence of strong downward solar radiation.

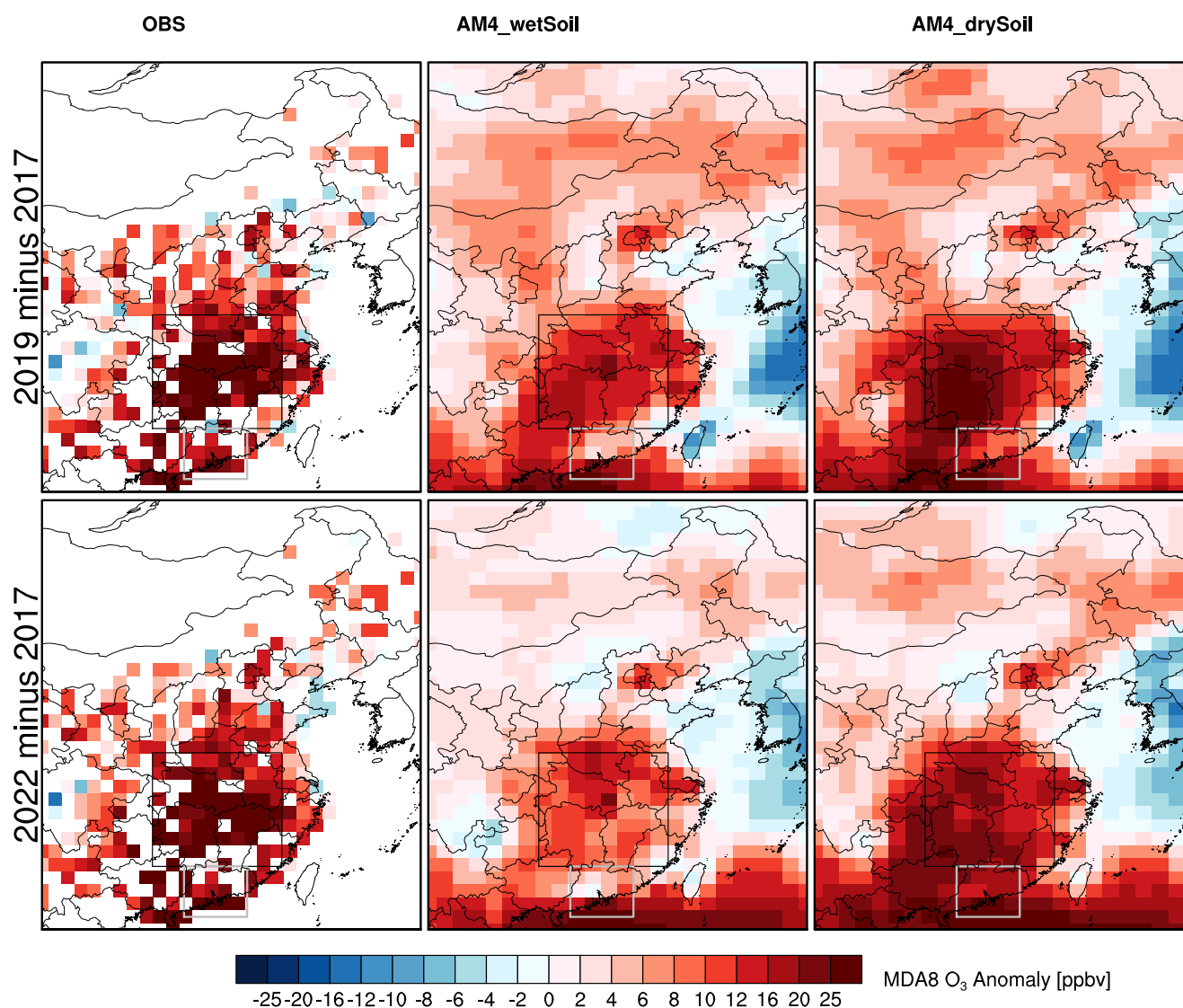


**Figure 5.** Anomalies in September mean surface MDA8 O<sub>3</sub> for 2019 and 2022 relative to 2017 from observations and two model simulations with changes in soil characteristics. The rectangles denote the Yangtze River Basin (black) and the Pearl River Delta (gray) analyzed in Figure 6.

Reductions in  $V_d$  of ozone precursors due to drought stress in vegetation also contribute to increased ozone production. Elevated ozone concentrations in Southeast China result not simply from transport of ozone suggested by some previous studies (e.g., Yang et al., 2024).

## 6. Impacts on Surface Ozone Concentrations

Finally, we quantify the extent to which biosphere-atmosphere interactions have influenced the observed ozone extremes during hot droughts. Observations show that September mean surface MDA8 O<sub>3</sub> in the YRB and the Pearl River Basin was 20–30 ppbv higher in 2019 and 2022 than 2017 (Figure 5). The two AM4 simulations with a different land state exhibit a striking contrast in their skill in representing the observed ozone anomalies. The AM4\_wetSoil simulation, which shows little change in  $V_{d,O_3}$  (Figure 2d), captures up to 50% of the observed ozone anomalies. With substantial reductions in ozone uptake by vegetation (Figure 2c) and increases in isoprene emissions due to warmer temperatures (Figure 4), AM4\_drySoil captures much better the magnitude and spatial pattern of observed high-ozone anomalies across Southeast China.



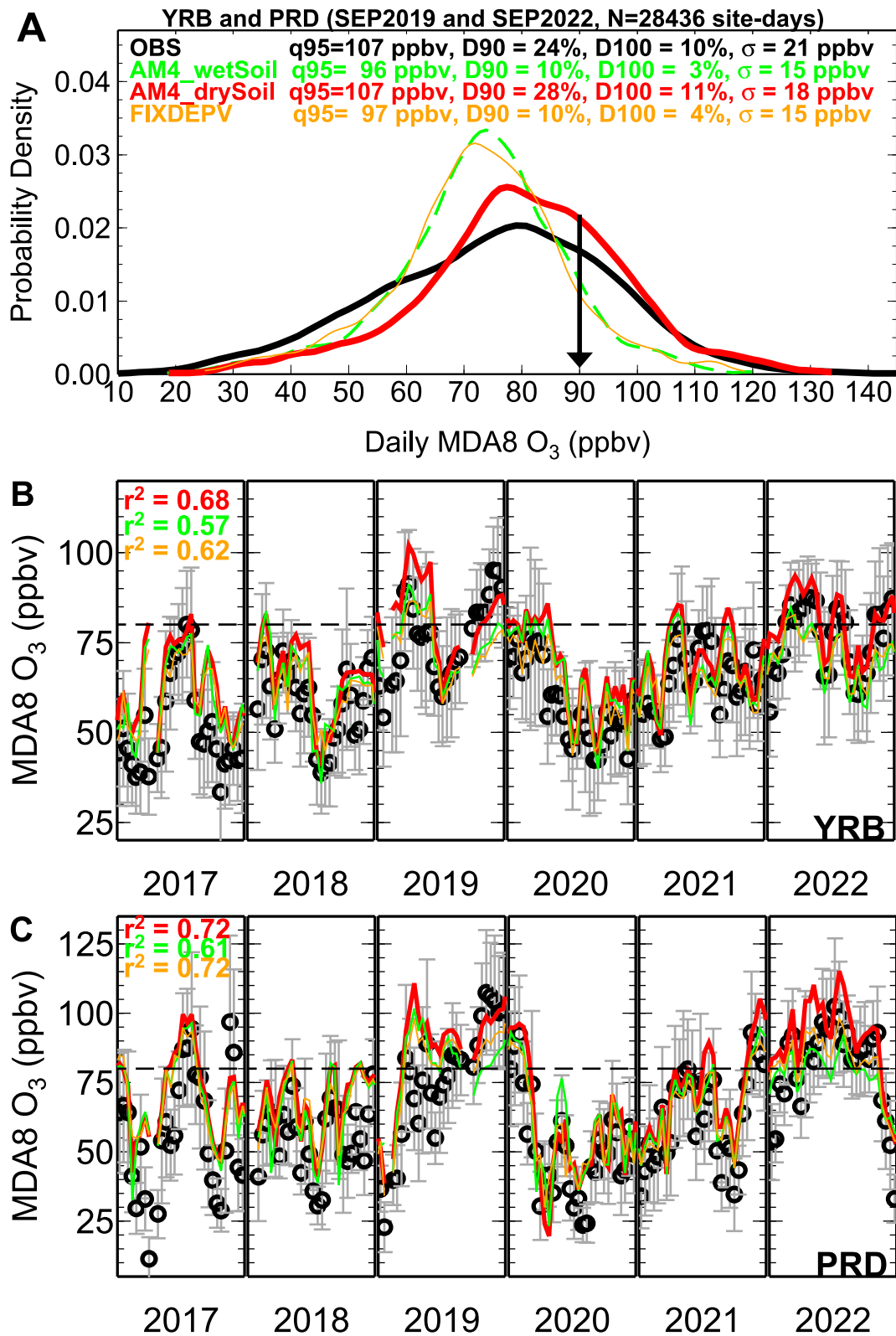


Figure 6.

The land-biosphere feedbacks exacerbate the most severe ozone events, causing an upward shift in the probability density distribution of daily MDA8 O<sub>3</sub> in Southeast China during hot droughts (Figure 6a). Results are also shown from the FIXDEPV simulation, in which soil characteristics follow AM4\_drySoil but V<sub>d</sub> of ozone and its precursors are prescribed at 2018 monthly values. Contrasting simulated MDA8 O<sub>3</sub> between AM4\_drySoil and FIXDEPV allows us to isolate the role of reduced ozone removal by vegetation. Since V<sub>d,O3</sub> in AM4\_wetSoil exhibits little interannual variability and is almost identical to the 2018 level used in FIXDEPV (Figure S3 in Supporting Information S1), we contrast MDA8 O<sub>3</sub> between AM4\_wetSoil and FIXDEPV to gauge the contribution from higher isoprene emissions and chemical rates resulting from warmer temperatures. We find that limitation in ozone removal due to drought stress in vegetation plays a dominant role in elevating ozone during compound drought and heat events in the Southeast. The number of events in which MDA8 O<sub>3</sub> exceeds 100 ppbv increases from 3% in AM4\_wetSoil to 4% in FIXDEPV and 11% in AM4\_drySoil, aligning with 10% in observations. Events above 90 ppbv increase from 10% in FIXDEPV (AM4\_wetSoil) to 28% in AM4\_drySoil, aligning with 24% in observations. Previous models have difficulties simulating observed peak ozone episodes (e.g., Gong et al., 2021; Yin et al., 2021). Here we show that accounting for the limitation in ozone uptake by drought-stressed vegetation, the distribution of ozone concentrations shifts toward that in observations. The 95th percentile of MDA8 O<sub>3</sub> in AM4\_drySoil matches the observed value (107 ppbv), increasing by 11 ppbv relative to AM4\_wetSoil and 10 ppbv relative to FIXDEPV. These impacts are significant, given that the Chinese National Ambient Air Quality Standard for MDA8 O<sub>3</sub> is 160 µg/m<sup>3</sup>, approximately 80 ppbv. During hot droughts, daily MDA8 O<sub>3</sub> can range from 80 to 130 ppbv for 10–20 consecutive days.

Satellite-derived HCHO-to-NO<sub>2</sub> ratios indicate a VOC-limited or transitional ozone production regime over megacity clusters in the North China Plain, the Yangtze River Delta, and the PRD, while a NO<sub>x</sub>-limited regime is found in less-developed, BVOC-rich areas in South China (Jin & Holloway, 2015; Ren et al., 2022). Our model also shows that ozone in South China responds (decreases) more strongly to 20% reductions in anthropogenic NO<sub>x</sub> than VOC emissions (Figure S8 in Supporting Information S1). Aligned with the NO<sub>x</sub>-limited ozone formation in South China, we find that a 27% increase in isoprene emissions in FIXDEPV (AM4\_drySoil) relative to AM4\_wetSoil have only marginal (<5 ppbv) impacts on ozone in the Yangtze Plain (orange vs. green lines in Figure 6b). In contrast, reductions in ozone removal by vegetation increased MDA8 O<sub>3</sub> concentrations by 10–20 ppbv during ozone episodes in 2022 (red vs. orange lines in Figure 6b). Over the PRD in 2022, total MDA8 O<sub>3</sub> change between AM4\_drySoil and AM4\_wetSoil is approximately 20 ppbv, for which warmer temperatures and increased isoprene emissions contribute 5–8 ppbv and reductions in ozone deposition contribute 8–15 ppbv (Figure 6c).

## 7. Implications for Ozone Air Quality Forecasting

Building upon our previous work for North America and Europe (Lin et al., 2019, 2020), this study highlights substantial reductions in ozone uptake by vegetation as a key mechanism driving recent ozone pollution extremes in Southeast China during hot droughts. As compound drought and heat events are projected to increase in a warming climate (e.g., L. Chen et al., 2023; Y. Zhang et al., 2024), a mechanistic understanding of ozone pollution during hot droughts is crucial to improve forecasting for public health alerts. Using a decade of observations and model simulations, we show that soil moisture deficits reduce ozone removal by vegetation, amplify heatwaves, and boost isoprene emissions. Including the effects of soil moisture deficits on ozone deposition and precursor emissions in models can improve forecasting of ozone extremes. Since soil moisture has longer persistence than atmospheric conditions, initialization of soil moisture using satellite observations in a coupled land–atmospheric chemistry model may increase the predictive lead time of ozone extremes and help with public health alerts in populated regions in China, North America and Europe.

**Figure 6.** (a) Probability density distribution of daily MDA8 O<sub>3</sub> in Southeast China for September 2019 and 2022 from observations (black) and three model simulations: AM4\_wetSoil (green), AM4\_drySoil (red), and FIXDEPV (orange, same as drySoil, but with fixed-2018 V<sub>d</sub>). The 95th percentile (q95), standard deviation (σ) and percentage of site-days with MDA8 O<sub>3</sub> exceeding 90 (D90) and 100 (D100) ppbv are shown. (b, c) Daily MDA8 O<sub>3</sub> during September from 2017 to 2022 in the Yangtze River Basin and the Pearl River Delta, respectively. Black dots represent the observed values averaged over sites in that region and gray bars represent cross-site standard deviation. Correlations (r<sup>2</sup>) between observations and model simulations are shown.

## Data Availability Statement

The source code of AM4 used in this study is identical to its variable-resolution version AM4VR, available at Lin (2023) and described in Lin, Horowitz, Zhao, et al. (2024).

## Acknowledgments

We thank John Dunne, Songmiao Fan, and Liwei Jia for helpful comments on this study. We are grateful to Luis Guanter for comments on the TROPOMI SIF products.

## References

- Beguieria, S., Vicente-Serrano, S. M., Reig, F., & Latorre, B. (2014). Standardized precipitation evapotranspiration index (SPEI) revisited: Parameter fitting, evapotranspiration models, tools, datasets and drought monitoring. *International Journal of Climatology*, 34(10), 3001–3023. <https://doi.org/10.1002/joc.3887>
- Chen, L., Li, Y., Ge, Z., Lu, B., Wang, L., Wei, X., et al. (2023). Causes of the extreme drought in late summer–autumn 2019 in eastern China and its future risk. *Journal of Climate*, 36(4), 1085–1104. <https://doi.org/10.1175/JCLI-D-22-0305.1>
- Chen, X., Huang, Y., Nie, C., Zhang, S., Wang, G., Chen, S., & Chen, Z. (2022). A long-term reconstructed TROPOMI solar-induced fluorescence dataset using machine learning algorithms. *Scientific Data*, 9(1), 427. <https://doi.org/10.1038/s41597-022-01520-1>
- Clifton, O. E., Fiore, A. M., Massman, W. J., Baublitz, C. B., Coyle, M., Emberson, L., et al. (2020). Dry deposition of ozone over land: Processes, measurement, and modeling. *Reviews of Geophysics*, 58(1), e2019RG000670. <https://doi.org/10.1029/2019rg000670>
- De Smedt, I., Pinardi, G., Vigouroux, C., Compennolle, S., Bais, A., Benavent, N., et al. (2021). Comparative assessment of TROPOMI and OMI formaldehyde observations and validation against MAX-DOAS network column measurements. *Atmospheric Chemistry and Physics*, 21(16), 12561–12593. <https://doi.org/10.5194/acp-21-12561-2021>
- Ding, T., Li, X., & Gao, H. (2022). An unprecedented high temperature event in southern China in autumn 2021 and the essential role of the mid-latitude trough. *Advances in Climate Change Research*, 13(6), 772–777. <https://doi.org/10.1016/j.accre.2022.11.002>
- Feng, Z., Xu, Y., Kobayashi, K., Dai, L., Zhang, T., Agathokleous, E., et al. (2022). Ozone pollution threatens the production of major staple crops in East Asia. *Nature Food*, 3(1), 47–56. <https://doi.org/10.1038/s43016-021-00422-6>
- Gong, C., Liao, H., Yue, X., Ma, Y., & Lei, Y. (2021). Impacts of ozone vegetation interactions on ozone pollution episodes in North China and the Yangtze River Delta. *Geophysical Research Letters*, 48(12), e2021GL093814. <https://doi.org/10.1029/2021GL093814>
- Guanter, L., Bacour, C., Schneider, A., Aben, I., van Kempen, T. A., Maignan, F., et al. (2021). The TROPOMI global sun-induced fluorescence dataset from the Sentinel-5P TROPOMI mission. *Earth System Science Data*, 13(11), 5423–5440. <https://doi.org/10.5194/essd-13-5423-2021>
- Guenther, A. B., Jiang, X., Heald, C. L., Sakulyanontvittaya, T., Duhl, T., Emmons, L. K., & Wang, X. (2012). The model of emissions of gases and aerosols from nature version 2.1 (MEGAN 2.1): An extended and updated framework for modeling biogenic emissions. *Geoscientific Model Development*, 5(6), 1471–1492. <https://doi.org/10.5194/gmd-5-1471-2012>
- Harris, I., Osborn, T. J., Jones, P., & Lister, D. (2020). Version 4 of the CRU TS monthly high-resolution gridded multivariate climate dataset. *Scientific Data*, 7(1), 109. <https://doi.org/10.1038/s41597-020-0453-3>
- Held, I. M., Guo, H., Adcroft, A., Dunne, J. P., Horowitz, L. W., Krasting, J., et al. (2019). Structure and performance of GFDL's CM4.0 climate model. *Journal of Advances in Modeling Earth Systems*, 11, 3691–3727. <https://doi.org/10.1029/2019MS001829>
- Helm, L. T., Shi, H., Lerdau, M. T., & Yang, X. (2020). Solar-induced chlorophyll fluorescence and short-term photosynthetic response to drought. *Ecological Applications*, 30(5), e02101. <https://doi.org/10.1002/eap.2101>
- Horowitz, L. W., Naik, V., Paulot, F., Ginoux, P. A., Dunne, J. P., Mao, J., et al. (2020). The GFDL global atmospheric chemistry-climate model AM4.1: Model description and simulation characteristics. *Journal of Advances in Modeling Earth Systems*, 12(10), e2019MS002032. <https://doi.org/10.1029/2019MS002032>
- Huang, L., McDonald-Buller, E. C., McGaughey, G., Kimura, Y., & Allen, D. T. (2016). The impact of drought on ozone dry deposition over eastern Texas. *Atmospheric Environment*, 127, 176–186. <https://doi.org/10.1016/j.atmosenv.2015.12.022>
- Jaffe, D. A., Cooper, O., Fiore, A., Henderson, B., Tonneson, G., Russell, T. R., et al. (2018). Scientific assessment of background ozone over the U.S.: Implications for air quality management. *Elementa: Science of the Anthropocene*, 6, 56. <https://doi.org/10.1525/elementa.309>
- Jin, X., & Holloway, T. (2015). Spatial and temporal variability of ozone sensitivity over China observed from the ozone monitoring instrument. *Journal of Geophysical Research: Atmospheres*, 120(14), 7229–7246. <https://doi.org/10.1002/2015JD023250>
- Li, K., Jacob, D. J., Liao, H., Zhu, J., Shah, V., Shen, L., et al. (2019). A two-pollutant strategy for improving ozone and particulate air quality in China. *Nature Geoscience*, 12(11), 906–910. <https://doi.org/10.1038/s41561-019-0464-x>
- Li, K., Jacob, D. J., Shen, L., Lu, X., De Smedt, I., & Liao, H. (2020). Increases in surface ozone pollution in China from 2013 to 2019: Anthropogenic and meteorological influences. *Atmospheric Chemistry and Physics*, 20(19), 11423–11433. <https://doi.org/10.5194/acp-20-11423-2020>
- Lin, M. (2023). Source code of AM4VR [Software]. *Zenodo*. <https://doi.org/10.5281/zenodo.10257866>
- Lin, M., Fiore, A. M., Horowitz, L. W., Cooper, O. R., Naik, V., Holloway, J., et al. (2012). Transport of Asian ozone pollution into surface air over the western United States in spring. *Journal of Geophysical Research*, 117(D21), D00V07. <https://doi.org/10.1029/2011JD016961>
- Lin, M., Holloway, T., Oki, T., Streets, D. G., & Richter, A. (2009). Multi-scale model analysis of boundary layer ozone over East Asia. *Atmospheric Chemistry and Physics*, 9(10), 3277–3301. <https://doi.org/10.5194/acp-9-3277-2009>
- Lin, M., Horowitz, L. W., Cooper, O. R., Tarasick, D., Conley, S., Iraci, L. T., et al. (2015). Revisiting the evidence of increasing springtime ozone mixing ratios in the free troposphere over western North America. *Geophysical Research Letters*, 42(20), 8719–8728. <https://doi.org/10.1002/2015GL065311>
- Lin, M., Horowitz, L. W., Hu, L., & Permar, W. (2024). Reactive nitrogen partitioning enhances the contribution of Canadian wildfire smoke plumes to U.S. ozone air quality. *Geophysical Research Letters*, 51(15), e2024GL109369. <https://doi.org/10.1029/2024GL109369>
- Lin, M., Horowitz, L. W., Payton, R., Fiore, A. M., & Tonneson, G. (2017). US surface ozone trends and extremes from 1980 to 2014: Quantifying the roles of rising Asian emissions, domestic controls, wildfires, and climate. *Atmospheric Chemistry and Physics*, 17(4), 2943–2970. <https://doi.org/10.5194/acp-17-2943-2017>
- Lin, M., Horowitz, L. W., Xie, Y., Paulot, F., Malyshev, S., Shevliakova, E., et al. (2020). Vegetation feedbacks during drought exacerbate ozone air pollution extremes in Europe. *Nature Climate Change*, 10(5), 444–451. <https://doi.org/10.1038/s41558-020-0743-y>
- Lin, M., Horowitz, L. W., Zhao, M., Harris, L., Ginoux, P., Dunne, J., et al. (2024). The GFDL variable-resolution global chemistry-climate model for Research at the Nexus of US climate and air quality extremes. *Journal of Advances in Modeling Earth Systems*, 16(4), e2023MS003984. <https://doi.org/10.1029/2023MS003984>
- Lin, M., Malyshev, S., Shevliakova, E., Paulot, F., W Horowitz, L., Fares, S., et al. (2019). Sensitivity of ozone dry deposition to ecosystem-atmosphere interactions: A critical appraisal of observations and simulations. *Global Biogeochemical Cycles*, 33(10), 1264–1288. <https://doi.org/10.1029/2018GB006157>

- Liu, H. Y., Jacob, D. J., Chan, L. Y., Oltmans, S. J., Bey, I., Yantosca, R. M., et al. (2002). Sources of tropospheric ozone along the Asian Pacific Rim: An analysis of ozonesonde observations. *Journal of Geophysical Research*, 107(D21), 4573. <https://doi.org/10.1029/2001JD002005>
- Liu, Y., Yuan, S., Zhu, Y., Ren, L., Chen, R., Zhu, X., & Xia, R. (2023). The patterns, magnitude, and drivers of the unprecedented 2022 mega-drought in the Yangtze River Basin, China. *Environmental Research Letters*, 18(11), 114006. <https://doi.org/10.1088/1748-9326/acfe21>
- Liu, Z., Doherty, R. M., Wild, O., Holloway, M., & O'Connor, F. M. (2021). Contrasting chemical environments in summertime for atmospheric ozone across major Chinese industrial regions: The effectiveness of emission control strategies. *Atmospheric Chemistry and Physics*, 21(13), 10689–10706. <https://doi.org/10.5194/acp-21-10689-2021>
- Liu, Z., & Zhou, W. (2021). The 2019 autumn hot drought over the middle-lower reaches of the Yangtze River in China: Early propagation, process evolution, and concurrence. *Journal of Geophysical Research: Atmospheres*, 126(15), e2020JD033742. <https://doi.org/10.1029/2020JD033742>
- Lu, X., Hong, J., Zhang, L., Cooper, O. R., Schultz, M. G., Xu, X., et al. (2018). Severe surface ozone pollution in China: A global perspective. *Environmental Science & Technology Letters*, 5(8), 487–494. <https://doi.org/10.1021/acs.estlett.8b00366>
- Ma, M., Gao, Y., Wang, Y., Zhang, S., Leung, L. R., Liu, C., et al. (2019). Substantial ozone enhancement over the North China Plain from increased biogenic emissions due to heat waves and land cover in summer 2017. *Atmospheric Chemistry and Physics*, 19, 12195–12207. <https://doi.org/10.5194/acp-19-12195-2019>
- Ma, M., Qu, Y., Lyu, J., Zhang, X., Su, Z., Gao, H., et al. (2022). The 2022 extreme drought in the Yangtze River Basin: Characteristics, causes and response strategies. *River*, 1(2), 162–171. <https://doi.org/10.1002/rvr2.23>
- Mao, J., Tai, A. P. K., Yung, D. H. Y., Yuan, T., Chau, K. T., & Feng, Z. (2024). Multidecadal ozone trends in China and implications for human health and crop yields: A hybrid approach combining a chemical transport model and machine learning. *Atmospheric Chemistry and Physics*, 24(1), 345–366. <https://doi.org/10.5194/acp-24-345-2024>
- Marengo, J., Nobre, C., Tomasella, J., Oyama, M., Sampaio de Oliveira, G., de Oliveira, R., et al. (2008). The drought of Amazonia in 2005. *Journal of Climate*, 21(3), 495–516. <https://doi.org/10.1175/2007jcli1600.1>
- Millet, D. B., Jacob, D. J., Boersma, K. F., Fu, T.-M., Kurosu, T. P., Chance, K., et al. (2008). Spatial distribution of isoprene emissions from North America derived from formaldehyde column measurements by the OMI satellite sensor. *Journal of Geophysical Research*, 113(D2), D02307. <https://doi.org/10.1029/2007jd008950>
- Milly, P. C. D., Malyshev, S. L., Shevliakova, E., Dunne, K. A., Findell, K. L., Gleeson, T., et al. (2014). An enhanced model of land water and energy for global hydrologic and Earth-system studies. *Journal of Hydrometeorology*, 15(5), 1739–1761. <https://doi.org/10.1175/jhm-d-13-0162.1>
- Moropoulos, C., Müller, J.-F., Stavrakou, T., Bauwens, M., De Smedt, I., Friedlingstein, P., et al. (2022). Vegetation responses to climate extremes recorded by remotely sensed atmospheric formaldehyde. *Global Change Biology*, 28, 1809–1822. <https://doi.org/10.1111/gcb.15880>
- National Environmental Satellite, Data, and Information Service (NESDIS 2024). (2024). STAR - global vegetation health products: High resolution (1km) vegetation health products from VIIRS. Retrieved from [https://www.star.nesdis.noaa.gov/smcd/emb/vci/VH/vh\\_1km.php](https://www.star.nesdis.noaa.gov/smcd/emb/vci/VH/vh_1km.php)
- Opacka, B., Müller, J.-F., Stavrakou, T., Miralles, D. G., Koppa, A., Pagán, B. R., et al. (2022). Impact of drought on isoprene fluxes assessed using field data, satellite-based GLEAM soil moisture and HCHO observations from OMI. *Remote Sensing*, 14, 2021. <https://doi.org/10.3390/rs14092021>
- Palmer, P. I., Jacob, D. J., Fiore, A. M., Martin, R. V., Chance, K., & Kurosu, T. P. (2003). Mapping isoprene emissions over North America using formaldehyde column observations from space. *Journal of Geophysical Research*, 108(D6), 4180. <https://doi.org/10.1029/2002jd002153>
- Paulot, F., Malyshev, S., Nguyen, T., Crounse, J. D., Shevliakova, E., & Horowitz, L. W. (2018). Representing sub-grid scale variations in nitrogen deposition associated with land use in a global Earth System Model: Implications for present and future nitrogen deposition fluxes over North America. *Atmospheric Chemistry and Physics*, 18(24), 17963–17978. <https://doi.org/10.5194/acp-18-17963-2018>
- Pu, D., Zhu, L., De Smedt, I., Li, X., Sun, W., Wang, D., et al. (2022). Response of anthropogenic volatile organic compound emissions to urbanization in Asia probed with TROPOMI and VIIRS satellite observations. *Geophysical Research Letters*, 49(18), e2022GL099470. <https://doi.org/10.1029/2022GL099470>
- Ren, J., Guo, F., & Xie, S. (2022). Diagnosing ozone–NO<sub>x</sub>–VOC sensitivity and revealing causes of ozone increases in China based on 2013–2021 satellite retrievals. *Atmospheric Chemistry and Physics*, 22, 15035–15047. <https://doi.org/10.5194/acp-22-15035-2022>
- Seco, R., Karl, T., Guenther, A., Hosman, K. P., Pallardy, S. G., Gu, L., et al. (2015). Ecosystem-scale volatile organic compound fluxes during an extreme drought in a broadleaf temperate forest of the Missouri Ozarks (central USA). *Global Change Biology*, 21(10), 3657–3674. <https://doi.org/10.1111/gcb.12980>
- Sharkey, T. D., & Monson, R. K. (2014). The future of isoprene emission from leaves, canopies and landscapes. *Plant, Cell and Environment*, 37(8), 1727–1740. <https://doi.org/10.1111/pce.12289>
- Shutter, J. D., Millet, D. B., Wells, K. C., Payne, V. H., Nowlan, C. R., & Abad, G. G. (2024). Interannual changes in atmospheric oxidation over forests determined from space. *Science Advances*, 10(20), eadn1115. <https://doi.org/10.1126/sciadv.adn1115>
- Teuling, A. J. (2018). Climate hydrology: A hot future for European droughts. *Nature Climate Change*, 8(5), 364–365. <https://doi.org/10.1038/s41558-018-0154-5>
- Trenberth, K., Dai, A., van der Schrier, G., Jones, P. D., Barichivich, J., Briffa, K. R., & Sheffield, J. (2014). Global warming and changes in drought. *Nature Climate Change*, 4(1), 17–22. <https://doi.org/10.1038/nclimate2067>
- Wang, D.-Q., & Sun, Y. (2022). Effects of anthropogenic forcing and atmospheric circulation on the record-breaking wet bulb heat event over southern China in September 2021. *Advances in Climate Change Research*, 13(6), 778–786. <https://doi.org/10.1016/j.accres.2022.11.007>
- Wang, N., Huang, X., Xu, J., Wang, T., Tan, Z.-M., & Ding, A. (2022). Typhoon-boosted biogenic emission aggravates cross-regional ozone pollution in China. *Science Advances*, 8(2). <https://doi.org/10.1126/sciadv.abl6166>
- Wang, N., Wang, H., Huang, X., Chen, X., Zou, Y., Deng, T., et al. (2024). Extreme weather exacerbates ozone pollution in the Pearl River Delta, China: Role of natural processes. *Atmospheric Chemistry and Physics*, 24(2), 1559–1570. <https://doi.org/10.5194/acp-24-1559-2024>
- Wang, P., Yang, Y., Li, H., Chen, L., Dang, R., Xue, D., et al. (2022). North China Plain as a hotspot of ozone pollution exacerbated by extreme high temperatures. *Atmospheric Chemistry and Physics*, 22(7), 4705–4719. <https://doi.org/10.5194/acp-22-4705-2022>
- Wang, T., Xue, L., Brimblecombe, P., Lam, Y. F., Li, L., & Zhang, L. (2017). Ozone pollution in China: A review of concentrations, meteorological influences, chemical precursors, and effects. *The Science of the Total Environment*, 575, 1582–1596. <https://doi.org/10.1016/j.scitotenv.2016.10.081>
- Wang, W., Parrish, D. D., Wang, S., Bao, F., Ni, R., Li, X., et al. (2022). Long-term trend of ozone pollution in China during 2014–2020: Distinct seasonal and spatial characteristics and ozone sensitivity. *Atmospheric Chemistry and Physics*, 22(13), 8935–8949. <https://doi.org/10.5194/acp-22-8935-2022>
- Wang, Y., McElroy, M. B., Munger, J. W., Hao, J., Ma, H., Nielsen, C. P., & Chen, Y. (2008). Variations of O<sub>3</sub> and CO in summertime at a rural site near Beijing. *Atmospheric Chemistry and Physics*, 8(21), 6355–6363. <https://doi.org/10.5194/acp-8-6355-2008>



- Wesely, M. L. (1989). Parameterization of surface resistances to gaseous dry deposition in regional-scale numerical models. *Atmospheric Environment*, 23, 1293–1304. [https://doi.org/10.1016/0004-6981\(89\)90153-4](https://doi.org/10.1016/0004-6981(89)90153-4)
- Xia, Y., Hu, Y., Huang, Y., Bian, J., Zhao, C., Wei, J., et al. (2022). Concurrent hot extremes and high ultraviolet radiation in summer over the Yangtze Plain and their possible impact on surface ozone. *Environmental Research Letters*, 17(6), 064001. <https://doi.org/10.1088/1748-9326/ac6c3c>
- Yang, Y., Zhou, Y., Wang, H., Li, M., Li, H., Wang, P., et al. (2024). Meteorological characteristics of extreme ozone pollution events in China and their future predictions. *Atmospheric Chemistry and Physics*, 24(2), 1177–1191. <https://doi.org/10.5194/acp-24-1177-2024>
- Yin, H., Lu, X., Sun, Y., Li, K., Gao, M., Zheng, B., & Liu, C. (2021). Unprecedented decline in summertime surface ozone over eastern China in 2020 comparably attributable to anthropogenic emission reductions and meteorology. *Environmental Research Letters*, 16(12), 124069. <https://doi.org/10.1088/1748-9326/ac3e22>
- Zhang, L., Yu, X., Zhou, T., Zhang, W., Hu, S., & Clark, R. (2023). Understanding and attribution of extreme heat and drought events in 2022: Current situation and future challenges. *Advances in Atmospheric Sciences*, 40(11), 1941–1951. <https://doi.org/10.1007/s00376-023-3171-x>
- Zhang, Q., Zheng, Y., Tong, D., Shao, M., Wang, S., Zhang, Y., et al. (2019). Drivers of improved PM2.5 air quality in China from 2013 to 2017. *Proceedings of the National Academy of Sciences of the United States of America*, 116(49), 24463–24469. <https://doi.org/10.1073/pnas.1907956116>
- Zhang, Y., Chen, L., Li, Y., & Ge, Z.-A. (2024). Anthropogenic influence on the extreme drought in eastern China in 2022 and its future risk. *Atmospheric and Oceanic Science Letters*, 17(1), 100390. <https://doi.org/10.1016/j.aosl.2023.100390>
- Zhao, M., Golaz, J., Held, I. M., Guo, H., Balaji, V., Benson, R., et al. (2018). The GFDL global atmosphere and land model AM4.0/LM4.0.2: Model description, sensitivity studies, and tuning strategies. *Journal of Advances in Modeling Earth Systems*, 10(3), 735–769. <https://doi.org/10.1002/2017ms001209>
- Zheng, Y., Unger, N., Tadić, J. M., Seco, R., Guenther, A. B., Barkley, M. P., et al. (2017). Drought impacts on photosynthesis, isoprene emission and atmospheric formaldehyde in a mid-latitude forest. *Atmospheric Environment*, 167, 190–201. <https://doi.org/10.1016/j.atmosenv.2017.08.017>